AUT Journal of Civil Engineering

AUT J. Civil Eng., 5(4) (2021) 643-656
DOI: 10.22060/ajce.2021.19518.5739

Lateral Stiffness and Bending Moment Changes along Piles Having Different Sections in Loose Sand Subjected to Cyclic Lateral Loading

A. Faresghoshooni, S. M. R. Imam*

Department of Civil and Environmental Engineering, Amirkabir University of Technology, Tehran, Iran.

ABSTRACT: Two-way cyclic lateral loading tests with constant displacement amplitude were performed on model piles in the sand to investigate the effects of cross-section geometry and modulus of elasticity on their behavior. The tested model pile sections included one square and three circular shapes and were made of polyethylene and polyurethane materials. The frequency of the cyclic loading was 0.29 Hz and the total number of loading cycles was 145 for all the tests. The model piles were tested in a metal test tank equipped with various facilities including a cyclic lateral loading system, devices to measure displacement and pressure along with the pile, an inverter to adjust or change loading frequency, a sand raining system, etc. Test results indicated that, from a global point of view, the soil modulus of lateral subgrade reaction and maximum moment developed in the pile increases with the number of loading cycles; however, the rate of increase gradually decreases. These variations may be formulated using a logarithmic relationship which includes a degradation parameter that reflects the rate of the mentioned decrease. It was also concluded that the cyclic effects are more significant for the lateral load resistance and stiffness than for the moment. The maximum moment at the 145th cycle for piles with various section geometries and elasticity moduli varied from 1.10 to 1.18 times the value obtained in the first cycle. Depending on the section shape and dimension, cyclic loading can increase the lateral stiffness of the soil at depths shallower than about 6.2 to 9.3 times the pile diameter.

Review History:

Received: Jan. 17, 2021
Revised: Sep. 11, 2021
Accepted: Sep. 19, 2021
Available Online: Apr. 01, 2022

Keywords:

Cyclic lateral load
Model test
Sand
Pile geometry
Lateral stiffness.

1- Introduction

Numerous studies have shown that the effect of cyclic loading on piles is a function of the number of cycles and characteristics of the applied load (see [1-5]) and various methods have been proposed to take into account these effects. The API and DNV design codes [6,7] apply a depth-dependent modification factor to modify the ultimate soil resistance based on the studies of Reese et al. [8] for the design of offshore structures. However, these modifications do not consider the effects of the number of loading cycles and characteristics of the applied load.

Bartolomey [9] studied the changes in the deformation modulus of the soil, the nature of the time-dependent pore pressure variations in the soil, and the other factors affecting the lateral behavior of piles both theoretically and experimentally. Field cyclic test data for piles installed in the sand were analyzed by Long and Vanneste [2] who found that cyclic loading affects the amount of pile deflection significantly. They found that the decrease in lateral stiffness and strength of piles in sands is more significant in one-way loading when compared to two-way loading. Based on results obtained from tests with less than two hundred loading cycles, they proposed correction factors for the lateral stiffness of sandy soils. Lin and Liao [3] reviewed earlier studies and proposed a new method based on field tests to reduce soil resistance using power law as a function of the number of cycles.

Several authors have proposed approaches for the determination of the effect of cyclic loading based on various theories and analyses (see [10,11]). Rosquoet et al. [4] investigated the change in tangent stiffness and the accumulation of displacement under lateral cyclic loading and observed that it varies approximately logarithmically. Based on the results of a series of small-scale centrifuge laboratory experiments on sand, Leblanc et al. [1] concluded that cyclic loading always increases soil-pile lateral stiffness, and this increase is independent of relative density. This conclusion is in contrast with the current methodology of decreasing static p-y curves to account for cyclic loading. They found that the accumulated rotation depends on the relative density and is strongly affected by the characteristics of the applied cyclic load and proposed a method to predict changes in stiffness due to long-term cyclic loading. Rudolph et al. [12] studied the effect of the direction of loading on the cyclic behavior of piles and concluded that the accumulation of displacement is significantly smaller when loading is applied in one direction compared to the case in which loading direction changes.

*Corresponding author's email: rimam@aut.ac.ir

Vahabkashi and Rahai [13, 14] showed that the stiffness of the pile-soil system increases with the increase in the loading cycles. Compared to piles with portions of their length extended above the ground surface, pile-soil system stiffness increase is higher when the entire pile length is embedded in the soil and the applied displacement at the pile head is greater. When piles are embedded in loose sand, the dissipation of energy is higher in the initial cycles and it decreases as the number of loading cycles increases.

Using results of centrifuge model tests, Truong and Lehane [15] examined the lateral loading behavior of displacement piles in soft kaolin and the effects of pile shape, pile end conditions, and clay over consolidation on the (p–y) curves. The tests were also modeled using the finite element method to compare the behaviors of the circular, square, and H pile sections used in the centrifuge tests. Both experimental and numerical results showed that the pile section shape has an important influence on the p–y curves. However, they observed no clear effect of the pile end condition on these curves. They also concluded that higher net pressures can develop against the square and H piles compared to circular piles since larger volumes of clay per unit pile width are involved in the failure mechanisms developed around the square and H piles.

Results of laboratory model tests on rigid monopiles in cohesionless soils subjected to lateral cyclic loading conducted by Abadie et al. [16] exhibited Masing behavior when the piles were subjected to symmetric cyclic loading. Results also showed some effects of the extended Masing behavior even after a large number of non-symmetric cyclic loading and, an increase in the accumulated ratcheting deformation due to non-zero mean applied load. The rate of ratcheting decreased with an increase in the number of cycles, however, it did not decrease to zero but it depended on the magnitude of the cyclic load. For the tests conducted by Abadie et al. [16], changes in the shape of the hysteresis loop shape in the form of an increase in the secant stiffness and decrease in the loop area occurred mainly during the first 50 cycles of loading.

A study of the behavior of large-diameter monopile foundations for offshore wind energy converters conducted by Frick and Achmus [17] showed that long-term cyclic lateral loading leads to an accumulation of permanent deflections and rotations of these monopolies. While these deflections and rotations should be limited to satisfy the serviceability criteria, predictions of their accumulation rates were found to be unreliable and difficult.

Displacement-controlled cyclic loading tests on a short steel monopole conducted by Darvishi Alamouti et al. [18] showed that the secant stiffness of the soil-pile system may increases, decrease, or remain constant depending on the applied cyclic displacements regime. These results are not consistent with the current design methodology in which only degradation is assumed to occur during cyclic loading. It was found that the influence of cyclic loading on the cyclic bending moments along the pile shaft is of minor significance.

Qin and Guo [19], Leblanc et al. [1], and Peng et al. [20] indicate that cyclic lateral loading of piles in the sand can compact the soil around the pile and increase the pile-soil stiffness. Considering these changes during the design of foundations such as those of turbines is essential since they affect the frequency of the turbine structural system and this has a significant effect on its response to dynamic loading.

While Leblanc et al. [1] reported only increases in soil-pile stiffness during cyclic loading in sandy soil, Klinkvort and Hededal [21] also observed decreases in stiffness for certain loading conditions. On the other hand, one-way, stress-controlled, cyclic lateral loading tests conducted by Chiou et al. [22] on a small-scale Aluminum pile in dry sand showed that the soil-pile stiffness decreases with an increase in the number of loading cycles.

Moreover, recent studies by Faresghoshooni et al. [23] showed that for tests with different pile cross-section shapes, dimensions, and moduli of elasticity, the pile head load and stiffness of the pile-soil system at the end of the 145th cycle varied from 1.4 to 1.85 times those of the first cycle for different section shapes, dimensions, and moduli of elasticity. Such effects have not been considered or quantified in current methodologies available for the design of piles subjected to cyclic loading.

In spite of the considerable research conducted in recent years on the cyclic behavior of piles, comprehensive data that can be used to provide general rules for considering the effects of many of the parameters that influence such behavior is still lacking. Besides, as indicated before, some of the results presented in current literature involve specific conditions or, are contradictory. Accordingly, general design rules have not yet been established or adopted in current design codes for considering soil-pile interaction issues, especially for short piles. It is, therefore, necessary to build a comprehensive database that includes the study of the effects of various soil and pile conditions such as different soil types and properties, different pile geometries, various loading patterns, etc. on pile behavior.

To compare the cyclic behavior of piles with different section geometries and moduli of elasticity, and to provide experimental data for use in proposing analytical relationships for displacement-controlled conditions, four experiments are conducted in the current study using small-scale pile models having different section geometries and made of polyethylene and polyurethane materials. The pile sections are subjected to two-way, constant displacement amplitude cyclic loading, and the overall response, such as the pile head load (given that the displacement amplitude is constant), stiffness of the pile-soil system, maximum moment, and p–y curves are investigated for the various cycles.

Faresghoshooni et al. [23] provided load-displacement model test results measured at the pile head and test data on changes in stiffness with the number of cycles relevant to the pile head for various pile cross-sections and moduli of elasticity. The mentioned results involved measurements only at the pile head. However, in the current study, based on measured loads and displacements at various depths along the pile length, changes in stiffness with the number of cycles are determined for various points along the pile length for different pile cross-section shapes and moduli of elasticity. Changes in

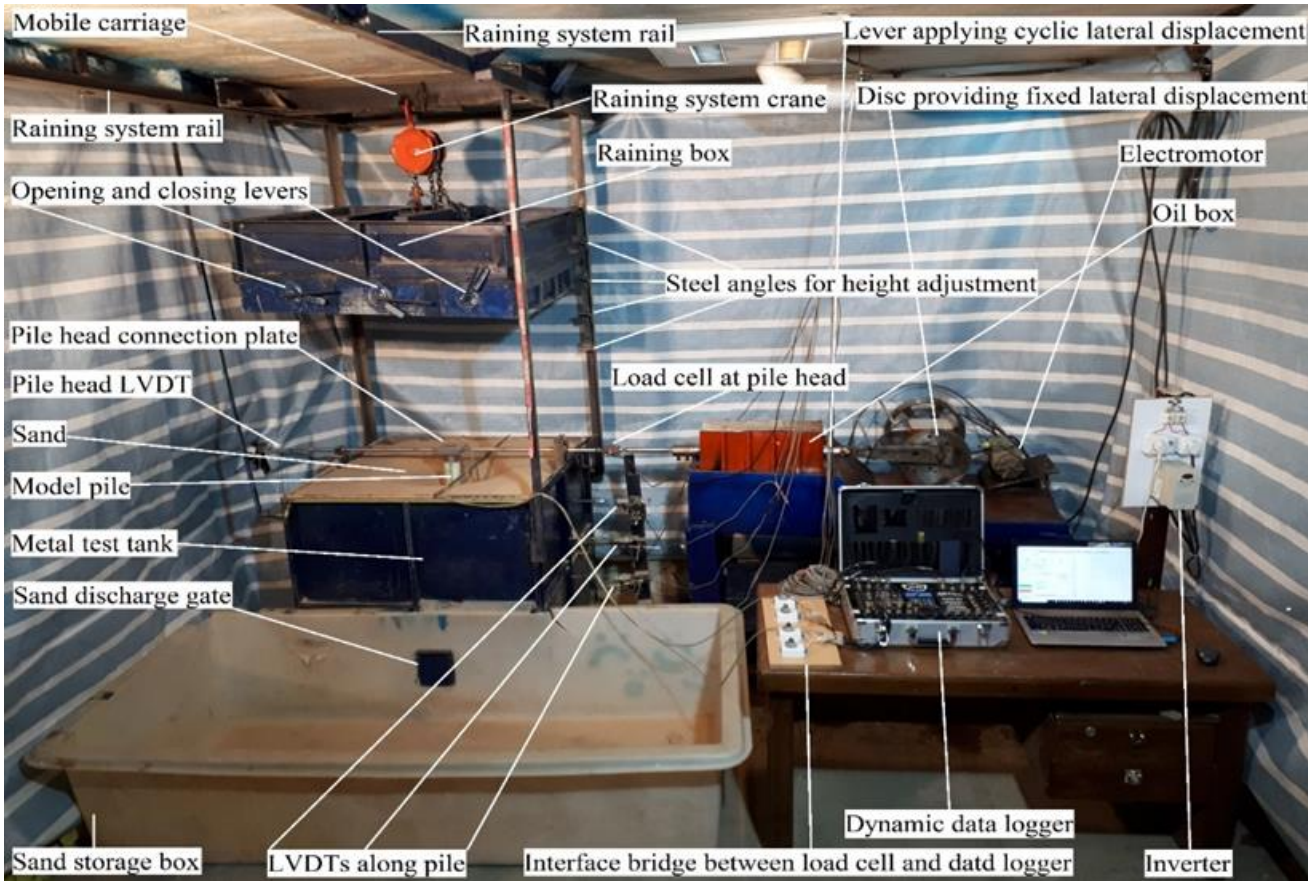

Fig. 1. Equipment used in the model testing of single piles.

the maximum moment induced in the pile with the number of loading cycles are also studied and results are shown and discussed for piles with various cross-section shapes and moduli of elasticity. It is expected that these results and the relationships derived from this data provide substantial assistance in formulating design rules applicable to piles subjected to cyclic loading for various conditions.

2- Testing Equipment and Setup

Model piles having 65mm wide square, and 65 and 74.2 mm circular sections were tested in a 1 × 1 × 1 m test tank filled with loose, dry sand placed by raining from a constant height of 1×1 m raining area. Considering that the largest dimension of the cross-section of the 880 mm long model piles was 74.2 mm, a distance of more than six times this dimension existed between the pile perimeter and the tank wall to minimize boundary effects. A relatively uniform, average relative density of 24.4 was achieved for the sand, which indicates that the sand was in a loose state. The use of loose sand in the model tests facilitates relating the results of these tests, which are conducted under low stresses, to the behavior of in situ piles, which are subjected to higher stresses. Considering the dilatancy characteristics of sands, loose sand subjected to low stresses behaves similarly to dense sand subjected to high stresses.

The lateral loading device was capable of applying loads at various constant frequencies and constant pile head displacement amplitudes. An inverter was used to adjust the loading frequency to 0.29 Hz (a period of 3.47 s) and the displacement amplitude was selected to be constant and equal to 48 mm and 76 mm for the different experiments. Various parts of the equipment used for conducting the cyclic lateral loading tests on the model piles are shown in Fig. 1 and details of the equipment and testing procedure are provided by Faresghoshooni et al. [23].

Test data was collected by several displacement sensors (LVDTs) and load cells mounted at five points selected at equal depth intervals along the pile length. A load cell was also used to measure changes in the pile head load during the constant displacement amplitude loading. A dynamic data logger was used to record the test data. It allowed ten readings per second and, given the cyclic loading period of 3.47 s, sufficient data points were recorded during loading to ensure relative continuity of the test results. A sketch of the pile and its instrumentation is shown in Fig. 2.

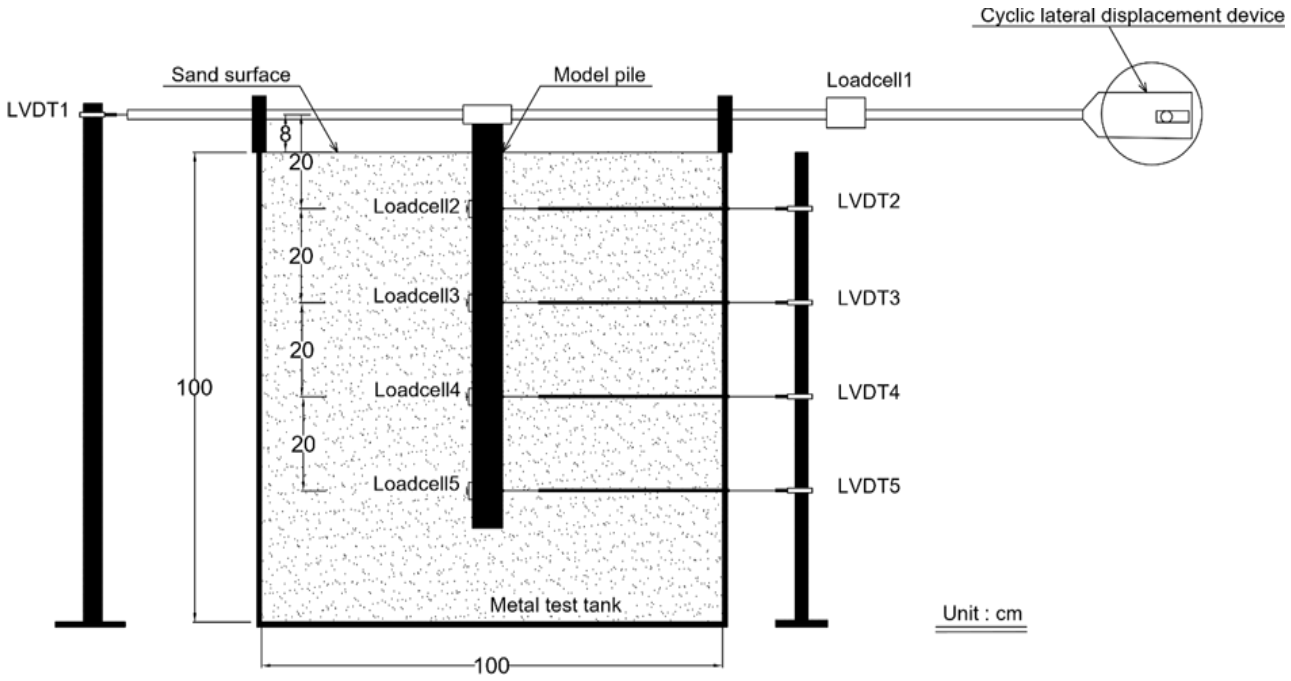

Fig. 2. A sketch of the instrumentation used in the model testing.

The dry sand used in the test is a local soil known as the Firoozkuh F161 sand produced by crushing parent rock. It is uniform fine sand of SP type according to the unified classification system ASTM D 2487 [24]. Its maximum and minimum void ratios are 0.931 and 0.58, respectively, and its mean void ratio D_{50} is 0.21 mm.

3- Specifications of the model piles

Internal forces and lateral displacements vary along the length of a laterally loaded pile, with greater changes typically occurring at shallower depths and smaller changes at greater depths. Depending on soil and pile properties, depths up to which greater changes of the mentioned variables occur vary, and piles in which these changes extend along most of the pile length are considered to be short piles. Piles may behave as short, long, or intermediate depending on the soil stiffness, and the pile moment of inertia, length, and modulus of elasticity. In the interpretation and application of the results of the tests conducted in the current study, it is important to determine whether the tested pile is considered as long, short, or intermediate so that the test results can be compared and applied to piles with similar conditions.

The model piles used in the current study were made of Polyethylene and Polyurethane and their cross-sections were either square or circular. Table 1 shows the four combinations of shapes and materials used in the tests conducted in the current study.

The same method was used for filling the test tank in all the tests and a sand relative density of 24.4 may therefore be assumed for all tests. The same embedded pile length of 880 mm was also used for all tests. Therefore, differences in the behavior of model piles were due to differences in the pile moment of inertia (cross-section shapes and dimensions) and the pile modulus of elasticity (pile material stiffness), the combination of which constitutes the pile flexural rigidity.

Matlock and Reese [25] indicated that piles may be considered as long (flexible) if $\frac{L}{T} \geq 5$ and short (rigid) if $\frac{L}{T} \leq 2$ where L is the pile length and T is its characteristic length defined as:

$$T = \sqrt[5]{\frac{E_p I_p}{n_h}} \quad (1)$$

In which E_p and I_p are the modulus of elasticity and moment of inertia of the pile section, respectively, and their values depend on the material, size, and shape of the pile cross-section, and n_h is the soil reaction modulus whose value for loose dry sand ranges from 1800 to 2200 kN/m^3 according to Matlock and Reese [25].

To determine the L/T ratio of the piles in various cases, the modulus of elasticity of the pile material should be obtained. This was done by conducting special tests on cantilever beams made of the pile material and measuring the beam deflection caused by loading it at its two ends as shown in Fig. 3.

Table 1. Specifications of sections of the pile models.

Test No.	*Cross-section*	*Material*	*Width or Diameter(mm)*	*Moment of inertia (m^4)*	*Section code*	$\frac{L}{T}$ *for* $n_{h\,(min)}$ *= 1800-2200*
1	Square	Polyethylene	65	1.49E-06	Sqr65	3.18-3.31
2	Circular	Polyethylene	65	8.76E-07	Circ65	3.54-3.68
3	Circular	Polyethylene	74.2	1.49E-06	Circ74.2	3.18-3.31
4	Circular	Polyurethane	65	8.76E-06	Circpu65	6.12-6.37

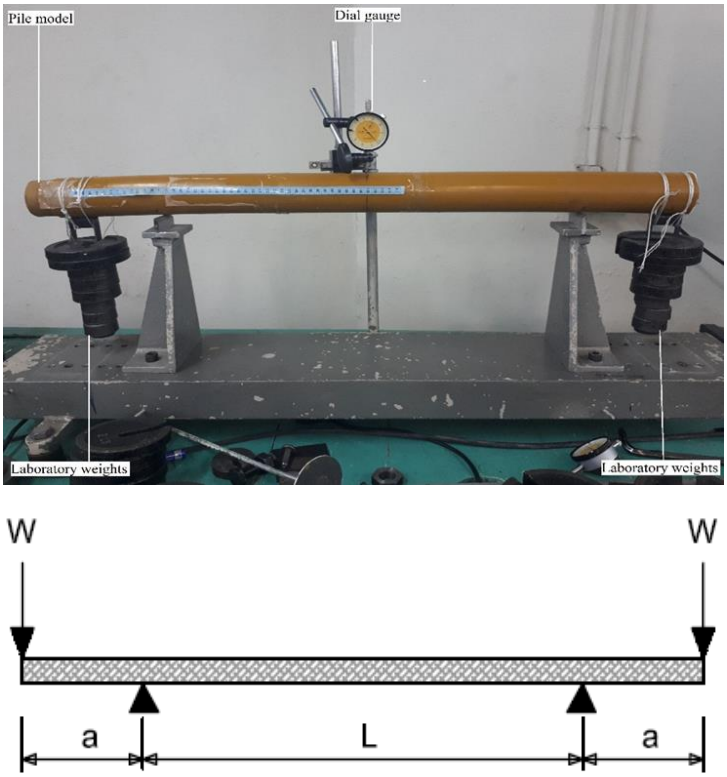

Fig. 3. Cantilever beam test setup used to obtain piles elastic moduli

Following the application of the point loads at the two free ends of the beam, the vertical deflection δ, in the middle of the beam span was measured. This deflection is related to the other parameters shown in Fig. 3 according to the following relationship:

$$\delta = \frac{WL^2a}{8EI} \qquad (2)$$

In the above equation, E is the modulus of elasticity of the material, and the values of a, L and W may be determined as shown in Fig. 3. By using different values of load and plotting the measured values of δ vs the applied loads W, the slope of the plot, which represents the pile stiffness ($K = \frac{W}{\delta}$) was determined and substituted in Eq. (2) to obtain the modulus of elasticity of the material.

Based on the results of the tests, moduli of elasticity of Polyethylene and Polyurethane were determined to be 1.96 and 0.126 GPa, respectively. Using the moduli of elasticity and dimensions of the model piles, flexural rigidities of the

piles and their behavior types were obtained. Considering the maximum and minimum values of n_h recommended by Matlock and Reese [25] for the sand tested as indicated before, characteristic length T values ranging from 0.239 to 0.277 m for the Polyethylene piles and from 0.138 to 0.144 m for the Polyurethane piles were obtained. Based on these results, ratios of L/H for the model piles were calculated as shown in Table 1. For the piles made of Polyethylene, this ratio ranged from 3.18 to 3.68 and these piles are therefore considered as having an intermediate length. For the pile made of Polyurethane, L/H values of 6.12 and 6.37 were obtained and this pile is therefore considered as being a long pile according to the Matlock and Reese [25] criteria.

It is noted that the mentioned designations of the tested piles as intermediate and long piles were obtained using values of reaction modulus applicable to the initial density of the soil, but this value may change upon cyclic loading due to densification of the surrounding soil. However, considering Eq. (1) and the values of the reaction modulus of denser sand, subsequent changes in this modulus are not expected to affect the designation of piles used in the current study.

4- Testing Method

Details of the testing procedure are provided by Faresghoshooni et al. [23] in which, the application of the two-way, constant displacement amplitude loading to the pile head is described in detail. Using the results of these tests, effects of the number of loading cycles, section shape, section dimensions, and pile modulus of elasticity on the soil-pile stiffness, soil pressure, maximum induced moment along the pile length, etc. were studied.

For each test, variations of pile head lateral load and displacement, and soil pressures and pile displacements at four locations along the pile length were recorded during loading. Using the data collected, changes in the soil-pile lateral stiffnesses, displacements, pressures, moments, and shear forces, and the p-y curves along the pile length were determined. All tests were conducted at a frequency of 0.29 Hz, which is considered slow and sufficiently low to prevent dynamic effects in the soil [26].

A pile may be subjected to approximately 10^7 loading cycles during its lifetime. Applying a large number of cycles is usually difficult and it is therefore common to carry out tests with a limited number of cycles and extrapolate the results for the numbers desired. In the current study, the number of cycles was limited to 145. The lateral displacement amplitude of the pile head is $Y_c = 48$ mm, which is at least 65% ($= \frac{Y_c}{D} = \frac{48}{74.2} = 0.65$) of the pile's largest dimension.

It is noted that the purpose of the current laboratory modeling is to analyze and compare behaviors of piles having different section geometries and elastic moduli rather than obtain values applicable to full-scale conditions. In this respect, the various section geometries and pile materials shown in Table 1 are used to compare the behavior of piles having different cross-sections and materials. A comparison of the behavior of circular and square piles with the same width and modulus of elasticity can be made by comparing results for sections Circ65 and Sqr65; a comparison of circular and square piles with the same flexural rigidity and modulus of elasticity can be made by comparing results from sections Circ74.2 and Sqr65, and comparison of circular sections with the same dimensions but with different moduli of elasticity can be made by comparing results from sections Circ65 and Circpu65.

5- Test Results

5- 1- Pile Moment profiles

The profile of induced moments along the pile length may be determined using the lateral displacement data (deflection curve) obtained from the measurements made at the five points along the pile length. Variations of the moment at any time during the tests may be calculated by differentiating the deflection curve twice.

Fig. 4 shows the profiles of moments at maximum lateral displacement along the pile length after a selected number of loading cycles is applied to the four pile sections tested. It may be seen that the profile of moments along with the pile initially increases relatively faster with the increase in the number of loading cycles, especially at the approximately 210mm and 570 mm depths, where the maximum positive and negative moments develop. The location of the maximum bending moment is at about z=210 mm, which corresponds to (2.8D) for Circ74.2 and (3.2D) for Sqr65, Circ65, and Circpu65. It may also be noticed that the maximum positive and negative bending moments along the pile lengths are very similar for the Circ74.2 and Sqr65 piles with the same flexural rigidity despite their different widths. However, the Sqr65 and Circ65 piles with the same width experience different maximum moments with the lower maximum moments induced in the circular section. On the other hand, the Circpu65 section experienced very low maximum moments due to the much smaller flexural rigidity despite its having the same section shape and width as the Circ65 section pile.

5- 2- Changes in the normalized maximum moment with the number of cycles

To examine changes in the pile maximum moment with the number of cycles for each test, variations of the maximum moment at the various loading cycles normalized to the maximum moment at the first cycle are calculated and plotted for various numbers of cycles as shown in Fig. 5. The figure shows the relationship between the $\frac{M_{max,N}}{M_{max,1}}$ ratio with the number of cycles for the various pile sections. $M_{max,1}$ and $M_{max,N}$ are the maximum moments of the pile head in the first and N^{th} cycles, respectively.

Fig. 5 shows that the normalized maximum moment increased with the increase in the number of loading cycles. Comparison with results reported by Faresghoshooni et al. [23] and those shown later in this section indicate that the degree of increase was less significant for the normalized moment compared to the pile head lateral load and stiffness of the pile-soil system. This finding is similar to that found by Garnier [27] and Chiou et al. [22].

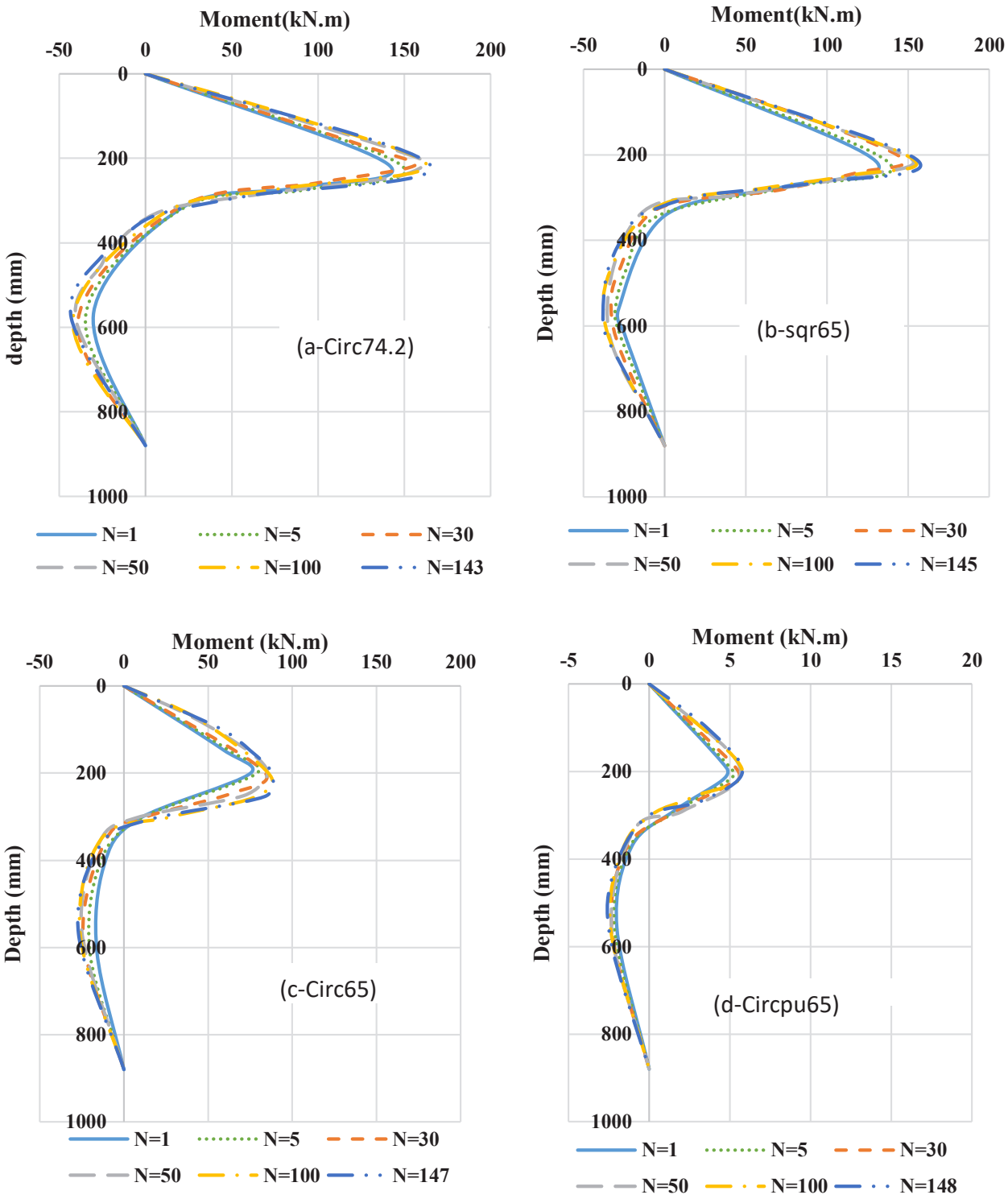

Fig. 4. Moment profiles at maximum displacement for the various pile sections and cycle numbers (numbers in legends indicate cycle number).

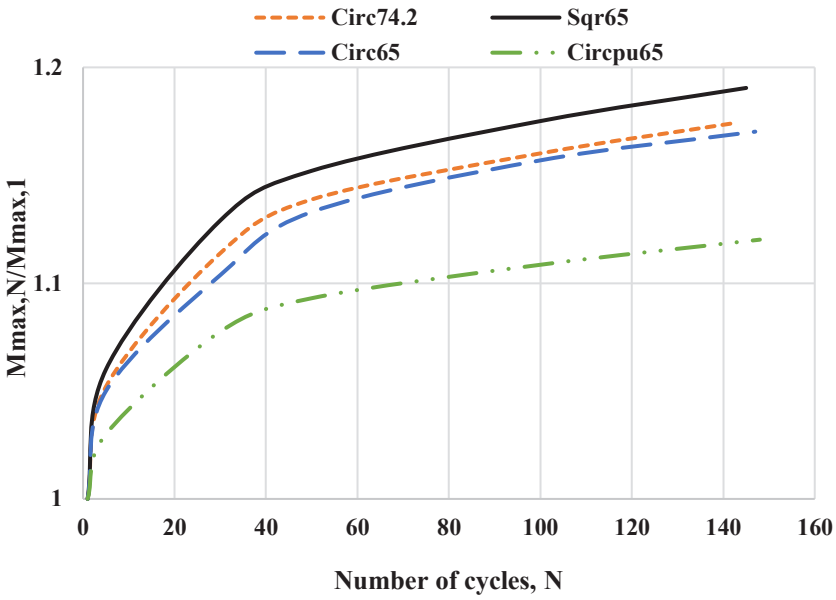

Fig. 5. Normalized maximum moment versus loading cycles.

Although all the pile sections were subjected to the same value of lateral displacement amplitude, Y_c, the increase in the maximum moment of the pile-soil system is seen to be influenced by the geometry and modulus of elasticity of the pile cross-section. From the plotted curves, it is shown that the maximum moment induced in the different pile sections at the end of the 145th cycle is 1.11 to 1.18 times greater than the maximum moment induced in the pile in the first cycle. This is equivalent to increases in a maximum moment of 11 to 18% due to the applied cyclic loading. These results indicate that the greatest increase in the normalized maximum moment occurred in the Sqr65 section and the least occurred in the Circpu65 section. The results also indicate that the normalized maximum moment of the Sqr65 and Circ65 piles having the same material and width (diameter) and moment of inertia ratio of 1.7 are 1.19 and 1.17, respectively. In other words, at the end of the cyclic loading, the increase in normalized pile maximum moment for the square section is about 2% greater than that of the circular section despite the relatively large difference in their moment of inertia (and therefore, their flexural rigidity).

On the other hand, for the Sqr65 and Circ74.2 piles having the same flexural rigidity and different widths, the normalized maximum moment values after 145 cycles are 1.19 and 1.18 respectively, indicating that the sections with the same flexural rigidity but different widths have a similar normalized maximum moment (about 1% greater increase in the square section) at the end of the cyclic loading. This indicates that the percent increase in maximum moment of the pile in loose sand during cyclic loading of piles made of the same material depends more on the moment of inertia (or flexural rigidity) of their section than on the pile width.

Comparison of results for the circular Circ65 and Circpu65 piles with a modulus of elasticity (and flexural rigidity) ratio of 15.55 and the same width and section moment of inertia shows that their normalized maximum moment after 145 loading cycles are 1.17 and 1.11, respectively, a difference of about 6%. This indicates that for piles with the same section shape and size but made of a material with different moduli of elasticity, the increase in the normalized maximum moment is greater for the pile with the greater elastic modulus (and flexural rigidity).

A comparison of the maximum moment increases for the three pairs discussed before indicates that the "increase" in the maximum induced moment in the piles due to cyclic loading depends mainly on the pile flexural rigidity EI (i.e., the product of moment of inertia and modulus of elasticity) rather than the section width, modulus of elasticity, or moment of inertia alone.

5- 3- Relationship of the normalized maximum moment with the number of cycles

In the displacement-controlled loading system used in this study, the following logarithmic relationship may be used for the variation of the ratio of the maximum moment in the N^{th} cycle to that in the first cycle, with the number of cycles:

$$\frac{M_{\max,N}}{M_{\max,1}} = 1 + cLn(N) \tag{3}$$

In which N is the number of cycles and c is a fitting parameter showing the rate of increase. By fitting the normalized

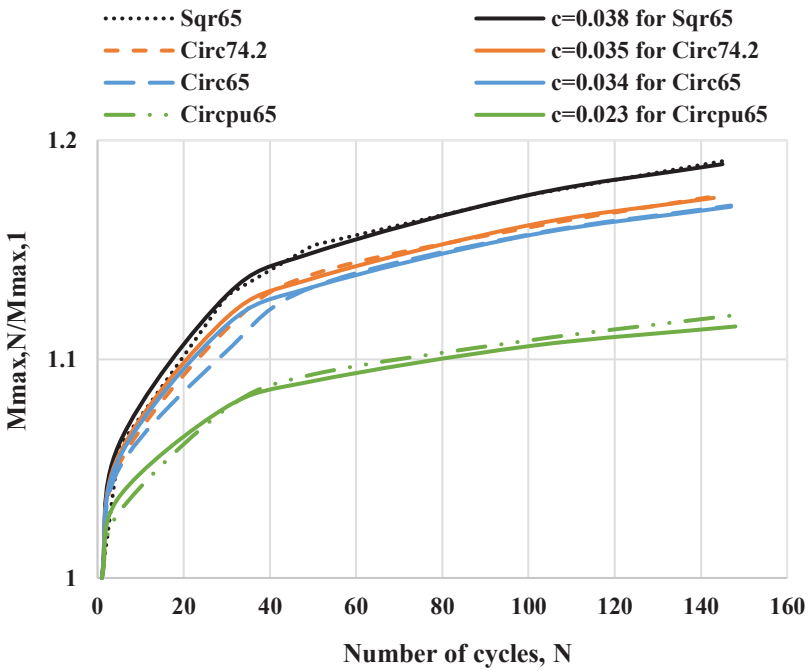

Fig. 6. Comparison of changes in the normalized maximum moment with the number of cycles obtained from tests with those from the proposed relationship for the various pile sections.

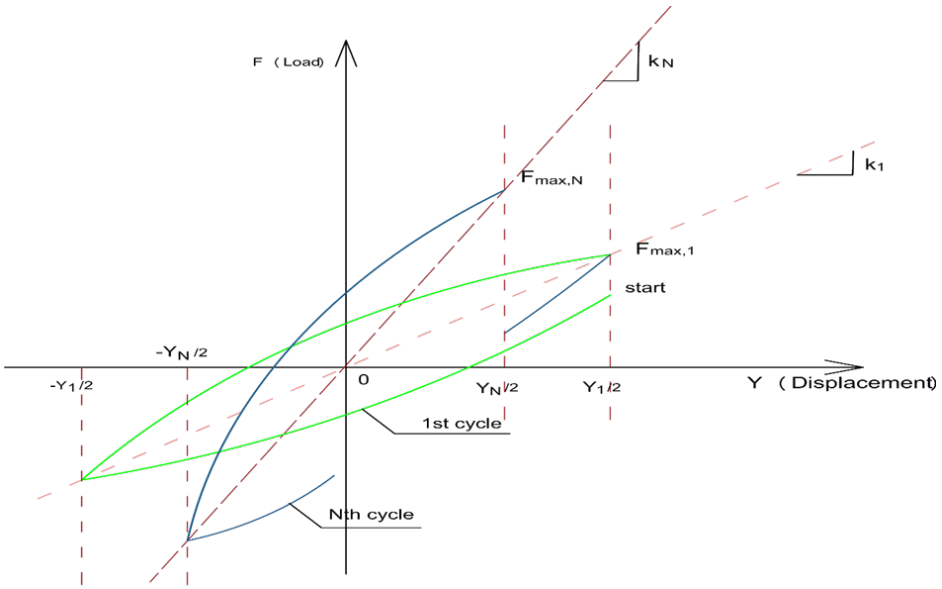

Fig. 7. Definition of the soil-pile stiffness obtained from a loading cycle.

maximum moment curves shown in Fig. 5 to Eq. (3), values of the parameter c for pile sections Sqr65, Circ74.2, Circ65, and Circpu65 are determined to be 0.038, 0.035, 0.034, and 0.023, respectively. A comparison of the fitted curves with the measured data is shown in Fig. 6. A comparison of the fitting parameters indicates that both the pile section geometry and modulus of elasticity affect the increase in the maximum moment due to cyclic loading rather than the width (or diameter) of the pile section, as indicated before.

5- 4- Variation of subgrade stiffness with the number of cycles

To investigate the lateral subgrade stiffness changes of the pile-soil system at different depths, the lateral subgrade stiffness of the pile-soil system in a cycle is defined here as the slope of the line passing through the minimum and maximum points on the load-displacement loop as shown in Fig. 7.

Based on the variations of the loads exerted on the pile, as measured at the locations of the load cells installed along the pile length, and the pile lateral displacement at those locations, the soil-pile stiffness curves were built at different depths in each test. Since the contact area between the load cell surface and the soil is constant and equal to 4 cm^2, the measured loads at various depths can be converted to pressures by dividing them into this contact area, and the ratios of pressure to displacement, which is the soil lateral subgrade reaction at that depth, can be determined. Therefore, variations of the stiffnesses discussed here also indicate the variations of lateral subgrade reaction of the soil at those depths.

Using the load-displacement curves obtained from the various tests, changes in stiffness during the loading cycles at different depths were determined. In Figs. 8 to11, the stiffness changes of the pile-soil system with the number of loading cycles for the different pile sections were normalized by dividing them by the stiffness of the pile-soil system in the first cycle. Similar to the behavior shown by Faresghoshooni et al. [23] for the pile head, the stiffness at depth below the soil surface increased with the increase in the number of loading cycles for piles Sqr65, Circ74.2, and Circ65. The curves indicate that at depths of 200 mm to 600 mm below the soil surface, the stiffness increased significantly, but for the depth below 600 mm, its increase was insignificant.

Comparison of results shown in Figs. 8 to 10 confirms that the rate of increase in stiffness with the number of loading cycles is greatest in Sqr65, followed by Circ74.2, and then Circ65. This may be due to the larger volume of soil in front of the pile being displaced and compacted (densified) in the square pile, followed by the circular pile with the higher diameter and then the pile with the lower diameter. The final increase in stiffness due to cyclic loading is also highest for Sqr65, for which a 70% increase in stiffness occurred at 200 mm depth below the soil surface at the end of the test. On the other hand, Fig. 11 shows that the pile with the smallest section modulus, the Circpu65, has experienced the smallest increase in stiffness at all depths, with less than 30% increase in stiffness at 200 mm depth below the soil surface. Comparison of stiffness changes with the number of cycles shown in Figs. 8 to 11 indicate that the rate of stiffness increase is higher in the initial loading cycles, and the rate of increase gradually decreases with the increase in the number of cycles. A clear change in the rate of increase occurs after about 40 to 60 loading cycles, after which this rate decreases significantly or reaches about zero, where further cyclic loading does not increase the stiffness anymore. This stage is reached earlier in the piles with the smaller section modulus such as the Circpu65 pile.

Figs. 8 to 11 can also be used to examine the rate of increase in stiffness with the increase in depth below the soil surface. All figures indicate that the final increase in stiffness, which occurs at the end test, decreases with the increase in depth below the soil surface. This is likely because of the decrease in amplitude of displacement during cyclic loading with depth, and the resulting decrease in soil densification at greater depths.

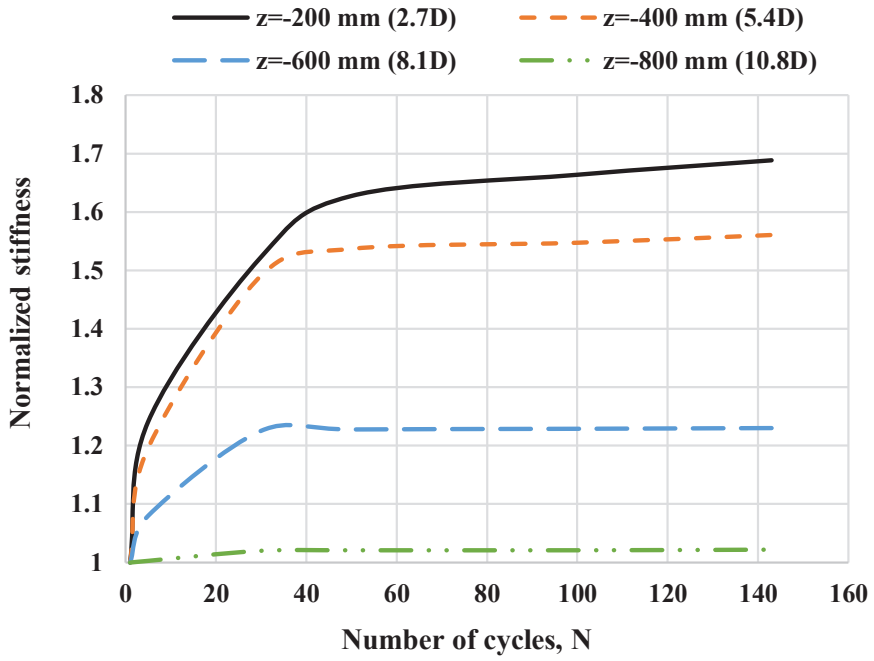

Fig. 8. Stiffness changes in the Circ74.2 section at various depths below the ground surface.

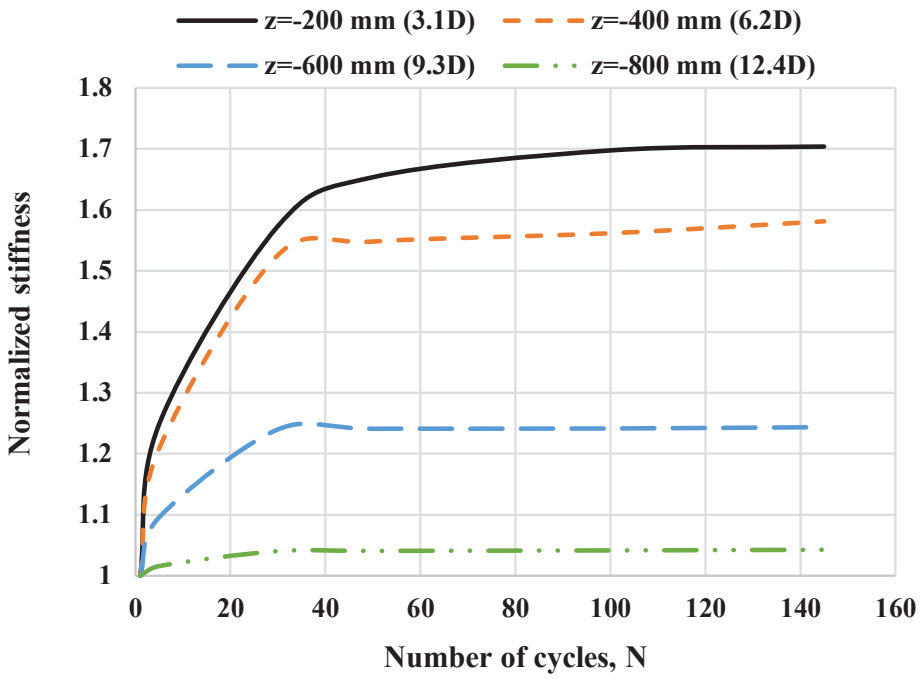

Fig. 9. Stiffness changes in the Sqr65 section at various depths below the ground surface.

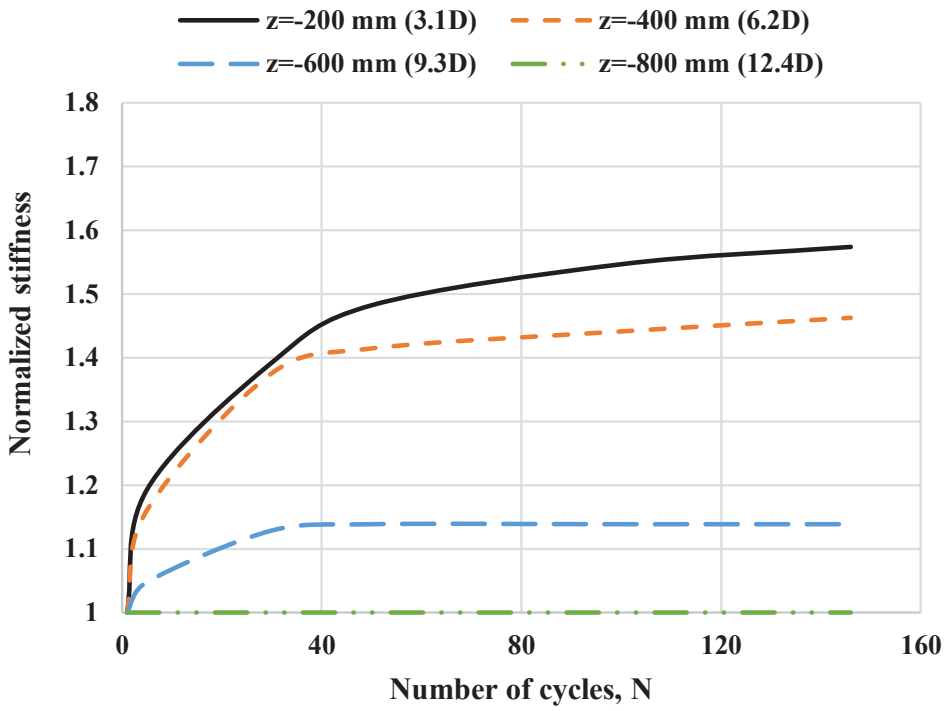

Fig. 10. Stiffness changes in the Circ65 section at various depths below the ground surface

dimensionless form and it is expected that the trends and general forms of variations obtained in the current study are also applicable to prototype, in-situ piles. However, numerical values of the parameters obtained for the proposed relationships may not be the same as those that may apply to full-scale conditions. Numerical values of such parameters applicable to in-situ conditions can be more accurately obtained from results of full-scale tests that are not easily carried out. Nevertheless, some guidelines in applying model test results to full-scale conditions using scaling effect considerations are briefly provided here. The reader is referred to relevant references such as that of Wood [29] for further details.

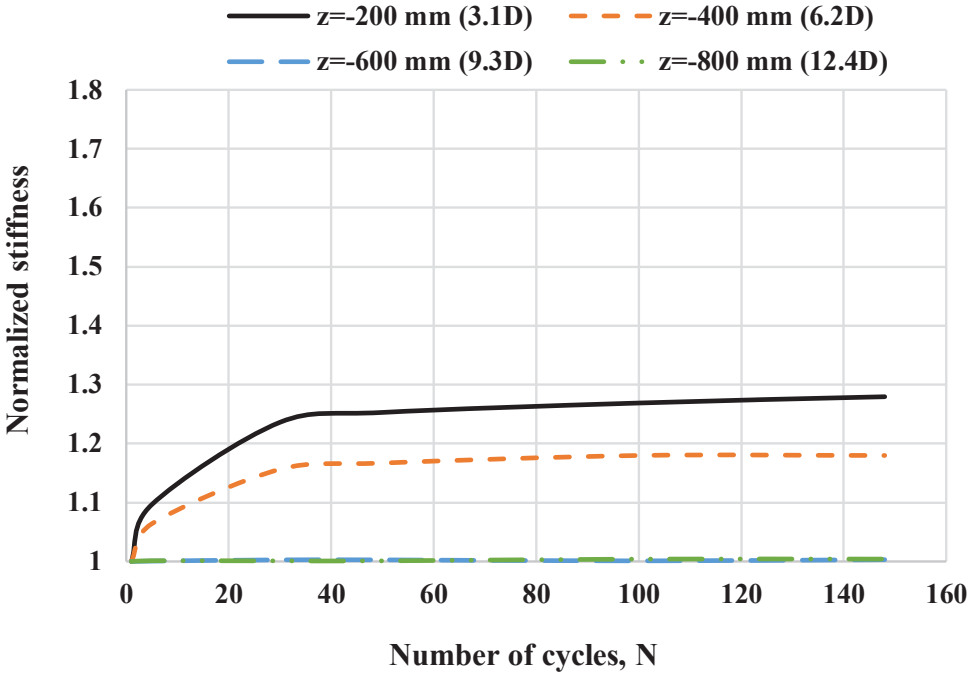

Fig. 11. Stiffness changes in the Circpu65 section at various depths below the ground surface.

5- 5- Depth of influence of various pile sections

An important aspect of pile behavior is its depth of influence, the depth below which the pile is no longer affected by the displacements or loadings that occur at shallower depths. Various researchers have reported different depths for the zone of influence, as a function of pile diameter, D. A value of 2.63D was reported by API [2], 4D by Reese, Cox, and Koop [1], and 5D by Garnier [27], and 7.5D by Chiou et al. [22]. It seems likely that this depth is also affected by soil density and pile stiffness, in addition to pile diameter.

From the test results shown, it was found that the mentioned depth of influence zone was about 8.1D for Circ74.2, 9.3D for Sqr65 and Circ65, and 6.2D for Circpu65. These differences in the influence zone may be due to the difference in the relative stiffness of the soil and pile. In general, the depth of the influence zone will be related to the depth range at which the pile exhibits its major response. For a pile-soil system, the major response of the pile is related to the characteristic length of the pile-soil system. According to Chiou and Chen [28] and Chiou et al. [22], the characteristic length is a function of the pile diameter and the modulus ratio of pile and soil. A larger pile diameter and a greater ratio of modulus of the pile to the soil will result in a deeper zone of influence for the pile-soil system.

5- 6- Application of test results to full-scale piles

In the model tests conducted in the current study, the size of the pile and stresses in its surrounding soil were significantly smaller than those of full-size, prototype piles. Results discussed in previous sections were presented in normalized,

If results obtained from the current study are to be applied to an in-situ pile with dimensions N times greater than those of the model pile, a variable obtained from the model tests should be multiplied by an appropriate factor, which depends on the parameters affecting that variable, to convert it to a value relevant to the full-scale condition. For example, stiffness in the small strain range may be considered to primarily depend on the square root of ambient stresses in granular soils [29]. In model tests, stresses are N times smaller than in-situ conditions. Therefore, small strain stiffness in in-situ conditions is approximately proportional to $N^{1/2}$ times the stiffness obtained from model tests. For medium strains, both stress and void ratio (density) affect stiffness; and, the combined effects may be taken into account using the concept of "state parameter, y" defined as the difference between the current void ratio and the void ratio at a critical state for the same mean effective stress. It is well known that soils having the same state parameter behave similarly and, therefore, looser soils subjected to low stresses behave similarly to denser soils

subjected to high stresses. This implies that to represent in-situ soils that are subjected to stresses higher than those in model tests, the void ratio in the model tests should be higher than that of the in-situ soil.

If the ratio of the model test to in-situ stresses is M, and the slope of the critical state line in the void ratio vs. logarithm of the mean effective stress plot is l, the difference in the void ratio of the soil used in the model tests and that of the in-situ soil should be Dt = l lnM. For example, for a pile with dimensions 20 times larger than the model pile (N = 20), stresses in the model test are 20 times smaller than in-situ stresses and M = 1/20. For a l = 0.03 for the tested Foroozkooh sand, the void ratio of the sand used in the model tests should be 0.09 higher than that of the in-situ soil. Considering the difference of 0.351 between the maximum and minimum void ratios of the tested sand as indicated in section 2, the sand with D_r = 24.4 used in model testing may be considered as representing an in-situ soil having a relative density of 0.256 greater than the tested soil, or soil with D_r = 50%. Similar analogies can be made for piles with dimensions having other ratios compared to the model pile, and for other studied variables.

6- Conclusion

Two-way cyclic lateral loading tests on model piles having different section geometries and material types were conducted in the current study. A total of four tests with a constant displacement amplitude of 48 mm were performed in test tanks filled with loose sand. A loading frequency of 0.29 Hz and a total number of loading cycles of 145 were used in all the tests. The following general conclusions may be derived from the results of the current study:

- The normalized maximum moment at the pile shaft at the 145th cycle for piles with various section geometries and elasticity moduli varied from 1.10 to 1.18 times the value obtained in the first cycle. An increase in the normalized maximum moment with the number of cycles may be shown by a logarithmic relationship and is greater for the pile with greater elastic modulus. The rate of increase was found to be higher during the first approximately 40 cycles and after about 100 cycles, it became very small or non-existent. Different rates of increase were observed for the various section geometries and elasticity moduli.
- For square and circular piles with the same width and diameter and elastic modulus, increases in normalized soil-pile stiffness at various depths and also in a maximum moment due to cyclic loading were greater for square piles compared to circular piles. This may be due to the larger volume of densified sand per unit pile width and the greater increase in density of the sand surrounding the square pile compared to the circular piles.
- Similar to the pile head behavior reported previously [23], at 200 mm to 600 mm depths below the soil surface, the pile-soil stiffness also increased with the number of cycles, but the rate and amount of increase were smaller at greater depths and higher cycle numbers. At depths greater than 600 mm, stiffnesses increased insignificantly with an increase in the number of cycles. The maximum depth of the influence zone for the subgrade stiffness varied from 6.2D to 9.3D below the soil surface for the piles with various section geometries and elastic moduli. Piles with larger diameters and ratio of the pile to soil modulus had deeper zones of influence.

Conflict of Interest Statement

All authors confirm that there is no conflict of interest regarding the publication of this paper.

References

[1] C. Leblanc, G.T. Houlsby, and B.W. Byrne, Response of stiff piles in sand to long-term cyclic lateral loading, Geotechnique, 60 (2) (2010) 79-90.

[2] J.H. Long, G. Vanneste, Effects of cyclic lateral loads on piles in sand, Journal of Geotechnical Engineering, 120 (1) (1994) 225-44.

[3] S.S. Lin, and J.C. Liao, Permanent strains of piles in sand due to cyclic lateral loads, Journal of Geotechnical and Geoenvironmental Engineering, 125(9) (1999) 789-802.

[4] F. Rosquoet, L. Thorel, J. Garnier and Y. Canepa, Lateral cyclic loading of sand-installed piles, Soils and Foundations, 47 (5) (2007) 821-832.

[5] R.T. Klinkvort, and O. Hededal, Lateral response of monopile supporting an offshore wind Turbine, Proceedings of the Institution of Civil Engineers: Geotechnical Engineering, 166(2) (2013) 147-158.

[6] API, Recommended practice for planning, designing and constructing fixed offshore platform, Working stress design, RP 2A-WSD, Washington, American Petroleum Institute, (2010).

[7] DNV, Rules for the design, construction, and inspection of offshore structures, Det Norske Veritas, Hovek, Norway, (1977).

[8] L.C. Reese, W.R. Cox, and F.D. Koop, Analysis of laterally loaded piles in sand, Proceeding of 6th Annual Offshore Technology Conference, Vol. 2, Houston, (1974) 473-484.

[9] A.A. Bartolomey, Forecast sediment pile foundations, Moskva, Stroiizdat, (1994) 390.

[10] K. Lesny, and P. Hinz Investigation of monopole behavior under cyclic lateral loading, In Proceeding of the 6th International Conference on Offshore Site Investigation and Geotechnics, London, (2007) 383-390.

[11] M. Achmus, Y. Kuo, and K. Abdel-Rahman, Behaviour of monopile foundations under cyclic lateral load, Computers and Geotechnics, 36(5) (2009) 725-735.

[12] C. Rudolph, B. Bienen, and J. Grabe, Effect of variation of the loading direction on the displacement accumulation of large-diameter piles under cyclic lateral loading in sand, Canadian Geotechnical Journal, 51(10) (2014) 1196-1206.

[13] P. Vahabkashi, A. Rahai, and A. Amirshahkarami, Lateral behavior of piles with different cross-sectional shapes under lateral cyclic loads in granular layered soils, International Journal of Civil Engineering, Transaction A: Civil Engineering, 12(1) (2014) 112-121.

[14] P. Vahabkashi, and A. Rahai, Pile head displacements with different cross-sectional shapes under lateral

loading and unloading in granular soils, Scientia Iranica, Transactions A: Civil Engineering, 22(3) (2015) 629-638.

[15] P. Truong, and B.M. Lehane, Effects of pile shape and pile end condition on the lateral response of displacement piles in soft clay, Géotechnique, 68(9) (2018) 794-804.

[16] C.N. Abadie, B.W. Byrne, and G.T. Houlsby, Rigid pile response to cyclic lateral loading: laboratory tests, Géotechnique, 69(10) (2019) 863-876.

[17] D. Frick, and M. Achmus, Model tests on the behavior of monopiles under general cyclic lateral loading, 2nd International Conference on Natural Hazards & Infrastructure, Chania, Greece, (2019).

[18] S. Darvishi Alamouti, M. Moradi, M.R. Bahaari, Centrifuge modeling of monopiles subjected to lateral loading, Scientia Iranica, Transactions A: Civil Engineering, 26(6) (2019) 3109-3124.

[19] H. Qin, and W. Guo, Response of static and cyclic laterally loaded rigid piles in sand, Marine Georesources and Geotechnology, 34 (2) (2016) 138-153.

[20] J. Peng, B.G. Clarke, M. Rouainia, Increasing the resistance of piles subject to cyclic lateral loading, Journal of Geotechnical and Geoenvironmental Engineering, 137(10) (2011) 977–982.

[21] R.T. Klinkvort, O. Hededal, and S.M. Springman, Scaling issues in centrifuge modeling of monopoles, International Journal of Physical Modelling in Geotechnics, 13(2) (2013) 38-49.

[22] J.S. Chiou, Z.W. Xu, C.C. Tsai, & J.H. Hwang, Lateral cyclic response of an aluminum model pile in sand, Marine Georesources and Geotechnology, 36(5) (2018) 554-563.

[23] A. Faresghoshooni, S.m.R. Imam, and A. Mahmoodi, Model testing on the effects of section geometry and stiffness on the cyclic lateral behavior of piles in loose sand, International Journal of Civil Engineering, (2020) 1-19.

[24] American Society for Testing and Materials. Standard Practice for Classification of Soils for Engineering Purposes (Unified Soil Classification System), ASTM D 2487, (2017).

[25] H. Matlock, and L.C. Reese, Generalized solutions for laterally loaded piles, Transactions of the American Society of Civil Engineers, 127(1) (1962) 1220-1247.

[26] J. Briaud, T. Smith, and L. Tucker, A pressuremeter method for laterally loaded piles, Proceeding of the eleventh international conference on soil mechanics and foundation engineering, San Francisco, (1985) 1353-1356.

[27] J. Garnier, Advances in lateral cyclic pile design, Contribution of the SOLCYP project, Proceedings of the TC 209 Work-shop, 18th ICSMGE-Design for Cyclic Loading: Piles and Other Foundations, Paris, (2013) 59-68.

[28] J.S. Chiou, and C.H. Chen, Exact equivalent model for a laterally loaded liner pile-soil system, Soil and foundations, 47(6) (2007) 1053-61.

[29] D.M. Wood, Geotechnical modeling, Version 2.2, (2004), CRC Press.

HOW TO CITE THIS ARTICLE

A. Faresghoshooni, S. M. R. Imam , Lateral Stiffness and Bending Moment Changes along Piles Having Different Sections in Loose Sand Subjected to Cyclic Lateral Loading , AUT J. Civil Eng., 5(4) (2021) 643-656.

DOI: 10.22060/ajce.2021.19518.5739